2019

Thermal performance of an evacuated tube heat pipe solar water heating system in cold season

Abdellah Sharifian
Edith Cowan University, a.shafieiandastjerdi@ecu.edu.au

Mehdi Khiadani
Edith Cowan University, m.khiadani@ecu.edu.au

Ataollah Nosrati
Edith Cowan University, a.nosrati@ecu.edu.au

10.1016/j.applthermaleng.2018.12.078
Shafieian, A., Khiadani, M., & Nosrati, A. (2018). Thermal performance of an evacuated tube heat pipe solar water heating system in cold season. *Applied Thermal Engineering, 149*, 644-657.
Available here.

Applied Thermal Engineering 149 (2019) 644–657

Contents lists available at ScienceDirect

Applied Thermal Engineering

journal homepage: www.elsevier.com/locate/apthermeng

Research Paper

Thermal performance of an evacuated tube heat pipe solar water heating system in cold season

Abdellah Shafieian, Mehdi Khiadani*, Ataollah Nosrati

School of Engineering, Edith Cowan University, 270 Joondalup Drive, Joondalup, Perth, WA 6027, Australia

HIGHLIGHTS

- The cold-season performance of a heat pipe solar water heating system was studied.
- Water consumption pattern plays a crucial role in optimum design of the system.
- Working fluid mass flow rate impacts on the outlet temperature and thermal efficiency.
- The highest thermal and exergy efficiencies were 92.7% and 15.58%, respectively.

ARTICLE INFO

Keywords:
Heat pipe collector
Solar water heating
Consumption pattern
Thermal efficiency
Exergy efficiency

ABSTRACT

This study evaluates the performance of a heat pipe solar water heating system to meet a real residential hot water consumption pattern theoretically and experimentally under non-ideal climatic conditions during a cold day in Perth, Western Australia. A mathematical model was developed and used to calculate the optimum number of glass tubes of the heat pipe solar collector. Based on the obtained data, an experimental rig with 25 glass tubes was designed, built, and tested as the temperature changes after 25 tubes reached the insignificant value of 0.6%. The results showed that hot water extraction had significant impact on the thermal performance of solar water heating system by increasing the amount of the absorbed energy and overall efficiency and decreasing exergy destruction. This indicates the importance of considering hot water consumption pattern in design and analysis of these systems. Auxiliary heating element was a necessary component of the system and played an important role mainly at the beginning of the operation in early morning (operation time of 19 min) and partly during the cloudy and overcast periods (operation time of 8 min). Two empirical equations relating the thermal and exergetic efficiencies of the heat pipe solar collector to the operational and environmental parameters were proposed. Comparison of the theoretical and experimental outlet temperature of the collector showed very good agreement with the maximum absolute and standard errors being 5.6% and 1.77%, respectively.

1. Introduction

Utilization of solar thermal systems is known as an effective method to face high energy demand and its consequent challenges and has a wide development potential. Solar water heating is the first and most common application of solar thermal systems [1]. Nonetheless, intractable challenges regarding effective collection and storage of solar energy pose significant limitations to its application [2]. This explains why solar collector is the most critical component of every solar heating system [3].

Heat pipe solar collectors (HPSCs) are a new type of solar collectors which can absorb and transfer solar energy more efficiently. These type of collectors have the advantages of both heat pipes and evacuated tube collectors [4]. Additionally, controlling operating temperature, overheating prevention, long operating lifetime, and also corrosion elimination are other advantages of HPSCs [5]. These unique advantages have turned HPSCs into an attractive option for solar domestic water heating systems [6].

Du et al. [7] prepared a platform for studying the performance of a HPSC in a solar water heating system. The obtained results including collector outlet temperature, instantaneous efficiency, and pressure drop were presented in details. The maximum achieved efficiency of the collector was 60% which occurred at the solar radiation of 860 W/m^2. Rassamakin et al. [8] proposed the application of specially extruded aluminium heat pipes in the HPSC of a solar water heating system to reduce the contact thermal resistance between the heat pipe and the

* Corresponding author.
E-mail addresses: a.shafieiandastjerdi@ecu.edu.au (A. Shafieian), m.khiadani@ecu.edu.au (M. Khiadani), a.nosrati@ecu.edu.au (A. Nosrati).

https://doi.org/10.1016/j.applthermaleng.2018.12.078
Received 1 August 2018; Received in revised form 7 November 2018; Accepted 12 December 2018
Available online 13 December 2018

Nomenclature

A	area (m^2)
a	air
ab	absorber
amb	ambient
C	specific heat capacity (J/kg K)
c	collector/condenser
d	diameter (m)
dest	destroyed
Ex	exergy rate (kW)
e	evaporator
F	radiation view factor
G	solar radiation intensity (W/m^2)
gi	inner glass
go	outer glass
h	heat transfer coefficient (convection) (W/m^2 K)/specific enthalpy (kJ/kg)
h_{fg}	latent heat of evaporation (J/kg)
h_p	heat pipe
i	internal/inner/inlet
i/in	inlet
k	thermal conductivity (W/mK)/location
L	length (m)/ liter
l	liquid
m	water flow rate (kg/s)
N	number
n	number
o	outer/ outlet
out	outlet
p	pipe
Q	heat transfer rate (W)
R	thermal resistance (K/W)
s	specific entropy (kJ/kg K)
T	temperature (K)
t	total/thickness (m)
v	vapor
W	work rate (W)
w	wick/water
0	dead state

Greek letters

η	efficiency
ε	emissivity/effectiveness
τ	transmittance
ρ	density (kg/m^3)
σ	Stefan Boltzman constant (5.670367×10^{-8} $kg/s^3 K^4$)
μ	dynamic viscosity (Pa s)
α	absorptivity
θ	angle

absorber. The results showed that the contact thermal resistance decreased to a great extent.

With the aim of increasing the heat transfer contact area of the HPSC of a water heating system, fin arrays were added to the condenser section of a HPSC [9]. A theoretical model was developed and its results were compared to experimental results. The results showed that the collector's thermal performance increased modestly by this method. Other methods to improve the performance of heat pipe solar heating systems include the application of compound parabolic concentrators (CPCs) [10–13], utilization of different solar working fluids (e.g., methanol, chloroform, ethanol, hexane, acetone, and petroleum ether) [14], use of integrated heat pipes instead of separate ones [15], and use of micro-channel heat pipes instead of separate heat pipes [16].

Kumar et al. [17] proposed a theoretical model to design a HPSC and study the heat transfer processes. According to the theoretical results, the effect of external conditions including solar radiation and ambient temperature on the thermal performance of HPSCs was more significant than other parameters. In addition, among all physical parameters, the collector was more sensitive to evaporator to condenser length ratio. Zhang et al. [18] characterized the energy transfer and conversion processes in a loop HPSC utilized in a solar water heating system. The developed theoretical model can be utilized to optimize the operational parameters and the geometrical configurations of the system. In a similar theoretical study, He et al. [19] studied the effect of heat pipe working fluid and external parameters on the thermal performance of a loop HPSC in a solar water heating system. It was found that higher solar radiation and ambient temperature had a positive effect on their proposed system's coefficient of performance.

The energy performance of a heat pipe solar water heating was studied in Dublin, Ireland by Ayompe and Duffy [20]. The mean daily collected energy was 20.4 MJ/d resulted in the solar fraction and system efficiency of 33.8% and 52.0%, respectively. In a similar investigation which focused on the extracted hot water from the solar storage tank, a heat pipe solar water heating system was studied in Spain. The results showed that there is a direct relation between the required water temperature and the system's efficiency [21].

Application of phase change materials (PCMs) in the HPSC's manifold section acting as the latent heat thermal energy storage was proposed Naghavi et al. [22]. Theoretical results showed that the proposed system reached higher efficiencies compared to the capability of operating efficiently at night or in low-radiation periods. In a similar study, Feliński and Sekret [23] proposed the application of PCMs inside the evacuated tubes of a heat pipe solar water heating system which increased the annual solar fraction of a domestic hot water system by 20.5%. Shafieian et al. [24] published a comprehensive review paper summarizing the utilization of HPSCs in various applications including domestic water heating systems.

Previous studies regarding heat pipe solar water heating systems have mainly focused on HPSC as a standalone component of the system, CPC heat pipe collectors, and more specifically thermal efficiency and thermal losses. In addition, most of the studies to date have not taken hot water consumption pattern into account while analysing a solar heating system without considering hot water discharge is far from actual operational conditions as it does not provide a comprehensive understanding of the system performance. Furthermore, most of the previous studies have not investigated the performance of heat pipe solar water heating systems in non-ideal climatic conditions with low solar radiation, cloudy and overcast periods, and low ambient temperature.

This study evaluated the performance of a heat pipe solar water heating system in a cold day while considering the hot water consumption pattern of Perth residents. Initially, a theoretical model was developed and the optimum number of glass tubes for a HPSC was obtained. Then, based on the theoretical results, an experimental rig was designed, built, and tested to evaluate the performance of the heat pipe solar water heating system. Moreover, the energetic and exergetic performance of the HPSC was investigated. Finally, the measured collector outlet temperatures were compared with the values calculated theoretically. The main novelties of the present study include analysing the performance of a HPSC in a solar heating system under real operational conditions, considering real residential water consumption pattern and evaluating its effect on the performance of the system, and studying the performance of a heat pipe solar water heating system under non-ideal climatic conditions of Australia in cold season.

2. Theoretical analysis of the HPSC

Theoretical study of the HPSC include analysis of solar collector, heat pipe, manifold, and exergy efficiency. The analysis was performed by using appropriate energy and exergy equations solved in Matlab software considering the following assumptions [6,25,26]:

- The heat loss from the manifold of the solar collector can be neglected.
- Temperature gradient in the longitudinal direction is negligible and only radial heat transfer is considered.
- The equations are in steady state and steady flow conditions.
- Contact resistance between heat pipes' wall and wick is negligible.
- The effects of kinetic and potential energies are negligible.
- No chemical and nuclear reactions exist.
- The specific heat capacity of water is constant.
- Heat transfer direction towards the system is positive.

2.1. Solar collector

The process of solar energy absorption and heat loss which occur in the solar collector and the associated thermal resistances is presented in Fig. 1. A portion of the solar radiation which strikes the glass is absorbed and used to vaporize the working fluid inside the heat pipes and the remainder is dissipated back into the environment. The vapor inside the heat pipes rises towards the condenser section where exchange its heat with the solar working fluid, condenses, and returns to the evaporator section, and the cycle continues.

The process of solar energy absorption and heat loss is described by the following thermal energy balance [27]:

$$Q_{ab} = Q_{en} - Q_{loss} \quad (1)$$

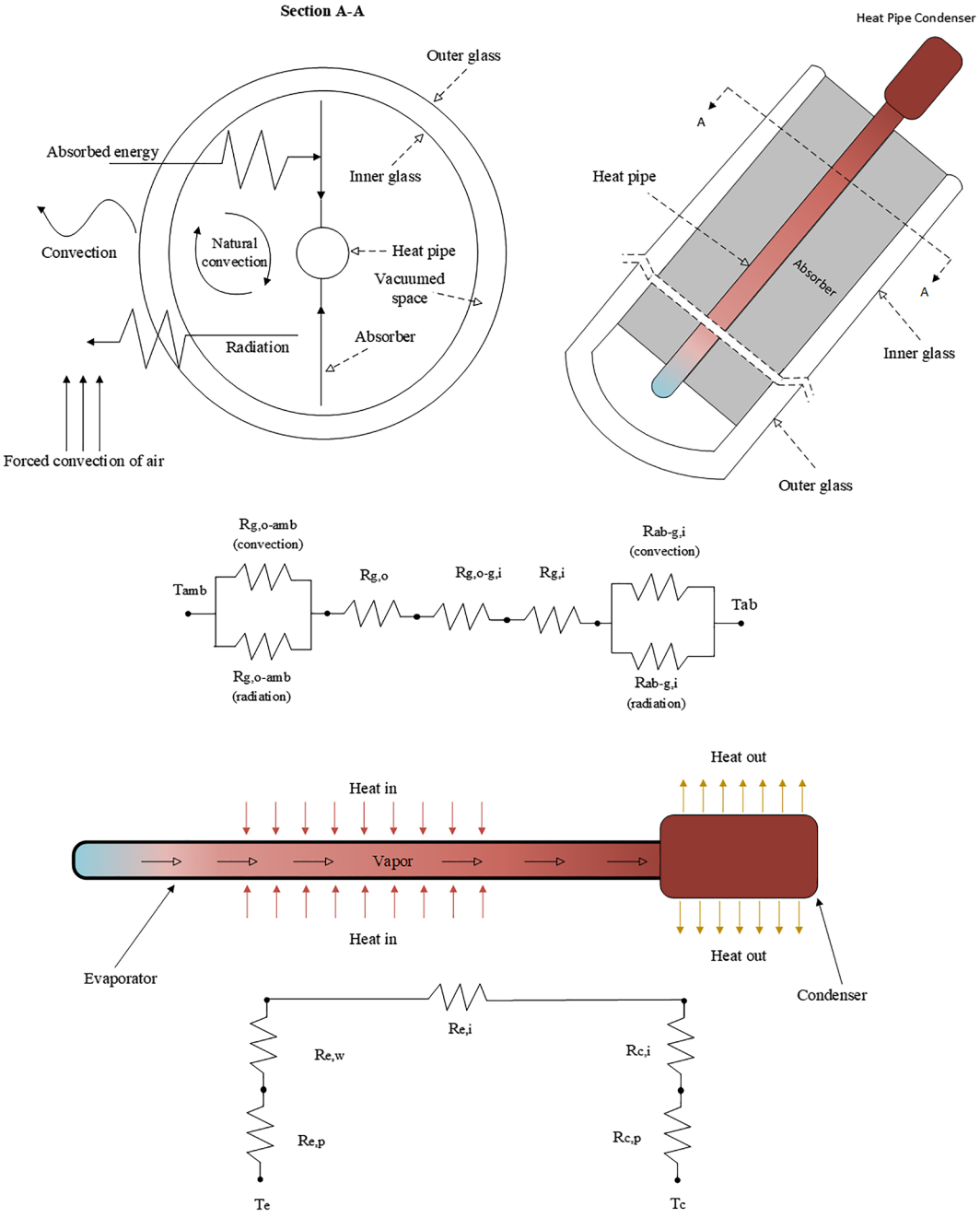

Fig. 1. Schematic diagram of the solar energy absorption and loss, thermal process inside a heat pipe along with the equivalent thermal resistances.

where Q_{ab} (W), Q_{en} (W), and Q_{loss} (W), are the absorbed thermal energy by the absorber surface, the solar energy passed through the glass tube, and the thermal energy which is dissipated back into the ambient, respectively. Q_{en} and Q_{loss} can be calculated from Eqs. (2) and (3), respectively [28,29].

$$Q_{en} = \tau_{go}\tau_{gi}\alpha_c A_{ab} N_{hp} G \tag{2}$$

$$Q_{loss} = \frac{T_{ab} - T_{amb}}{R_t} \tag{3}$$

where τ_{go}, τ_{gi}, and α_c are the transmittance of the outer glass, the transmittance of the inner glass, and the absorptivity of the absorber surface, respectively. In Eq. (3), T_{ab} (°C) is the absorber temperature, T_{amb} (°C) is the ambient temperature, and R_t (K/W) is the summation of all the thermal resistances shown in Fig. 1 including the natural convection and radiation resistances between the absorber and the inner glass ($R_{ab\text{-}gi}$), the conduction resistance of the inner glass (R_{gi}), the radiation resistance between the inner and outer glass ($R_{gi\text{-}go}$), the conduction resistance of the outer glass (R_{go}), and the forced convection and radiation resistances between the outer glass and ambient ($R_{go\text{-}amb}$). They can be obtained from Eqs. (4)–(8) [29,30].

$$R_{ab-gi} = \frac{1}{h_a\left(\frac{A_{ab}+A_{gi}}{2}\right)} + \frac{\frac{1-\varepsilon_{ab}}{\varepsilon_{ab}A_{ab}} + \frac{1}{A_{ab}F_{ab-g}} + \frac{1-\varepsilon_{gi}}{\varepsilon_{gi}A_{gi}}}{\sigma(T_{ab}+T_{gi})(T_{ab}^2+T_{gi}^2)} \tag{4}$$

$$R_{go-amb} = \frac{1}{A_g}\left(\frac{1}{h_{amb}} + \frac{1}{\sigma(T_{go}+T_{amb})(T_{go}^2+T_{amb}^2)}\right) \tag{5}$$

$$R_{gi-go} = \frac{\frac{1-\varepsilon_{gi}}{\varepsilon_{gi}A_{gi}} + \frac{1}{A_{gi}F_{gi-go}} + \frac{1-\varepsilon_{go}}{\varepsilon_{go}A_{go}}}{\sigma(T_{gi}+T_{go})(T_{gi}^2+T_{go}^2)} \tag{6}$$

$$R_{gi} = \frac{t_{gi}}{k_{gi}A_{gi}} \tag{7}$$

$$R_{go} = \frac{t_{go}}{k_{go}A_{go}} \tag{8}$$

where h (W/m^2 K), A (m^2), F, T (°C), t (m), k (W/mK) are convective heat transfer coefficient, area, view factor, temperature, thickness, and thermal conductivity, respectively.

2.2. Heat pipe heat transfer

The total thermal resistance of a heat pipe (R) defines as the summation of several resistances (Fig. 1) including the evaporator wall resistance ($R_{e,p}$), the wick resistance ($R_{e,w}$), the internal resistance ($R_{e,i}$), the condenser resistance ($R_{c,i}$), and the condenser wall resistance ($R_{c,p}$) can be calculated from Eq. (9) [31].

$$R = R_{e,p} + R_{e,w} + R_{e,i} + R_v + R_{c,i} + R_{c,p} \tag{9}$$

The evaporator wall resistance ($R_{e,p}$), the wick resistance ($R_{e,w}$), and the internal resistance ($R_{e,i}$) are calculated from Eqs. (10)–(12), respectively [32].

$$R_{e,p} = \frac{\ln\left(\frac{d_o}{d_i}\right)}{2\pi k_p L_e} \tag{10}$$

$$R_{e,w} = \frac{\ln\left(\frac{d_{o,w}}{d_{i,w}}\right)}{2\pi k_w L_e} \tag{11}$$

$$R_{e,i} = \frac{2}{h_e \pi d_i L_e} \tag{12}$$

The effective thermal conductivity of the wick structure, k_w (W/mK), in Eq. (11) can be obtained from [33]:

$$k_w = \frac{k_l[k_l + k_s - (1-\varepsilon_w)(k_l - k_s)]}{k_l + k_s + (1-\varepsilon_w)(k_l - k_s)} \tag{13}$$

The film coefficient of the internal resistance, h_e (W/m^{2}K), in Eq. (12) can be written as [34]:

$$h_e = \frac{k_l}{t_w} \tag{14}$$

The conduction wall resistance of the condenser can be expressed as [32]:

$$R_{c,p} = \frac{\ln\left(\frac{d_o}{d_i}\right)}{2\pi k_p L_c} \tag{15}$$

The thermal resistance regarding the condensation process of the working fluid can be calculated from [32]:

$$R_{c,i} = \frac{1}{h_{c,i}\pi d_i L_c} \tag{16}$$

where, $h_{c,i}$ (W/m^{2}K) is the heat transfer coefficient of the condensation process and can be expressed as [32]:

$$h_{c,i} = 0.728\left[\frac{g sin\theta \rho_l(\rho_l - \rho_v)k^3 h_{fg}}{D\mu_i \Delta T_i}\right]^{0.25} \tag{17}$$

where g (m/s^2), θ (°), ρ (kg/m^3), h_{fg} (J/kg), and μ (Pa s) are the gravitational acceleration, the inclination angle, the density, the latent heat of evaporation, and the dynamic viscosity, respectively.

2.3. Manifold

In a HPSC, the solar working fluid reaches the first heat pipe in the manifold section with the highest temperature difference with the heat pipe condenser. The solar working fluid absorbs thermal energy and its temperature rises while it moves towards the next heat pipe. Consequently, the outlet cooling fluid temperature of each heat pipe equals to the inlet temperature is of the next one.

Considering the reality that a condensation process at almost a constant temperature occurs inside the condenser section of heat pipes, the effectiveness-NTU (Number of Transfer Units) method [32] can be applied to determine the outlet temperature of solar working fluid after each heat pipe ($T_{o,n}$) from:

$$T_{o,n} = T_{i,n} + \varepsilon_n(T_{c,n} - T_{i,n}) \tag{18}$$

where $T_{i,n}$, $T_{c,n}$, and ε_n are the inlet temperature, the condensor temperature, and the effectiveness of the nth heat pipe, respectively.

The collector efficiency (η_c) can be determined from [26]:

$$\eta_c = \frac{m_w C_w (T_{w,o} - T_{w,i})}{GA_c} \tag{19}$$

where m_w (kg/s), C_w (J/kgK), $T_{w,o}$ (°C), and $T_{w,i}$ (°C) are the mass flow rate of the working fluid, heat capacity, the collector outlet temperature, and the collector inlet temperature, respectively.

2.4. Exergy efficiency

In this study, exergy analysis is performed to provide an overview of the magnitude and time of high energy losses and to determine the opportunities for thermodynamic enhancement. Through this process, the factors influencing the thermodynamic imperfection of the system can be identified and evaluated quantitatively for efficient design of energy systems. In solar systems, the solar collector has the highest irreversibility (exergy destruction) [35].

The exergy balance equation can be defined as [25]:

$$\sum Ex_{in} - \sum Ex_{out} = Ex_{dest} \tag{20}$$

which can be expanded to [25]:

$$\sum \left(1 - \frac{T_o}{T_k}\right) Q_k - W + \sum m_{in}\varphi_{in} - \sum m_{out}\varphi_{out} = Ex_{dest} \tag{21}$$

where φ (kJ/kg), Q (kW), and W (kW) are the physical exergy flow, heat transfer rate, and work rate, respectively. The physical exergy flow is defined as [25]:

$$\varphi_{in/out} = (h_{in/out} - h_0) - T_0(s_{in/out} - s_0) \tag{22}$$

where h (kJ/kg), s (kJ/kgK), and T_0 (K) represent specific enthalpy, specific entropy, and temperature at dead state, respectively. Exergy efficiency of the system can be expressed as [35]:

$$\eta_{sc} = \frac{Ex_u}{Ex_{sc}} \tag{23}$$

where Ex_u (kW) is the useful delivered exergy and Ex_{sc} (kW) is the collector absorbed exergy and can be calculated from Eq. (24) or (25), and Eq. (26), respectively [35].

$$Ex_u = m_w[(h - h_0) - T_0(s - s_0)] \tag{24}$$

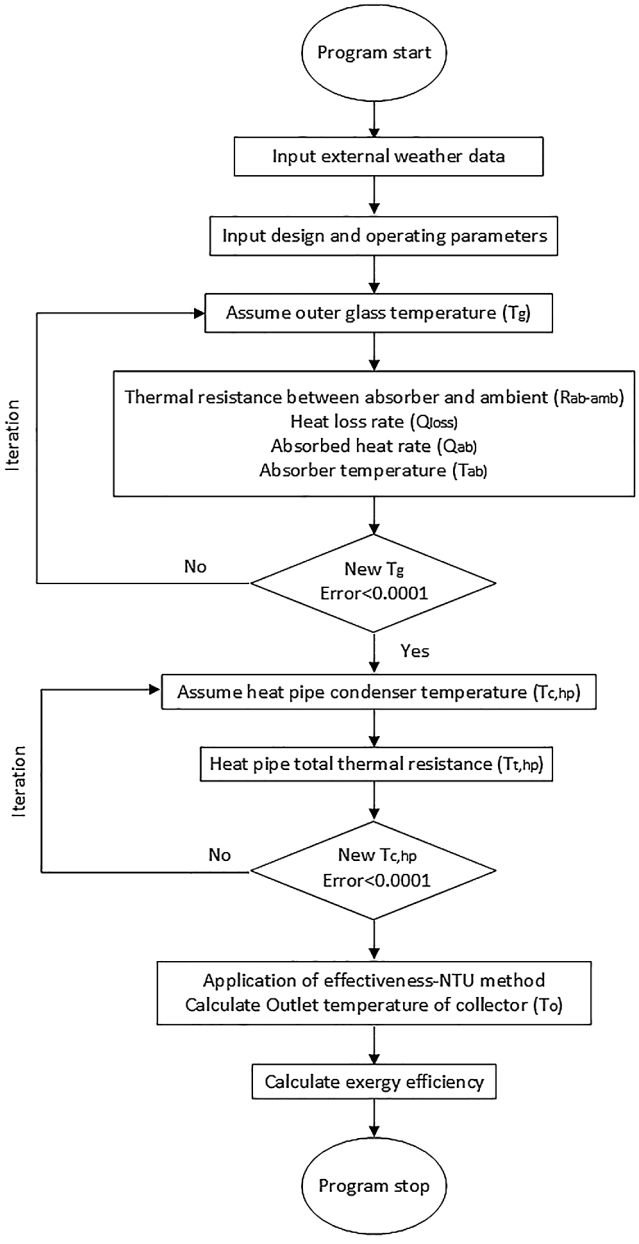

Fig. 2. The flowchart of developed theoretical model.

$$Ex_u = m_w C_w[(T_o - T_i) - T_0\left(\ln\frac{T_o}{T_i}\right)] \tag{25}$$

$$Ex_{sc} = AG\left[1 + \frac{1}{3}\left(\frac{T_o}{T_{sr}}\right)^4 - \frac{4}{3}\left(\frac{T_o}{T_{sr}}\right)\right] \tag{26}$$

where T_{sr} and C_w (J/kgK) are the solar radiation temperature which is equal to 6000 K and specific heat capacity, respectively.

Fig. 2 illustrates the algorithm of computation process used in this study for modelling the HPSC.

3. Experimental setup and instrumentation

3.1. Experimental setup description

Fig. 3 shows the components of the proposed heat pipe solar water heating system. The system mainly consists of heat pipe solar collector; water storage tank; central control unit (including a control unit, a National Instrument Data Acquisition (NI-DAQ) system, and a computer); thermocouples; pump; flow meter; pipes and fittings; and valves.

A portion of the solar radiation which strikes the glass of HPSC is absorbed and used to vaporize the working fluid inside the heat pipes and the remainder is dissipated back into the environment. The vapor inside the heat pipes rises towards the condenser section where transfers its heat to the solar working fluid through the manifold, condenses, and returns to the evaporator section, and the cycle continues. The solar working fluid, which is circulated using a pump, enters the manifold at low temperature and its temperature rises as it passes along the manifold. The heated solar working fluid then passes through the copper coil to exchange its heat with the water inside the tank. Heated water is extracted from the top of the storage tank at 60 °C based on the hot water consumption pattern and replaced with tap water from the bottom of the storage tank.

A pump (Davey Company) was used to circulate the solar working fluid in the solar loop. The flow rate of the solar working fluid (distilled water) was regulated via a valve installed after the pump. The low temperature solar working fluid (2 l/min) entered the manifold and its temperature was raised as it passed over the heat pipe condensers. The heated solar working fluid then passed through a 34 m copper coil (with external heat transfer area of 1.45 m^2) which was installed inside a 210-liter storage tank to exchange its heat with the water inside the tank. The storage tank was insulated with a 50-mm layer of thermal insulation materials. The hot water was extracted from the storage tank at 60 °C based on the hot water consumption pattern of a residential house. This was done using a manual valve and the volume of extracted water was collected in a scaled container. An auxiliary heater (2 KW) was also installed inside the storage tank to heat the water to 60 °C when the solar radiation was low and the heat pipe solar collector was not able to provide all the required energy (e.g., early mornings and during cloudy periods).

Seven thermocouples (Type: T- Class1 made by TC Ltd.) were installed and monitored with a NI-DAQ system to measure the temperatures at various locations of the system. An application program interface (API) was programmed in the LabVIEW 2014 software to record the data at 10-second intervals. Climatic data including solar radiation, ambient temperature, and wind velocity were collected from the weather station located at Edith Cowan University, Joondalup Campus which is located 23 km north of Perth business district.

The heat pipe solar collector was purchased from Century Sun Energy Technology Company in China and its specifications are presented in Table 1.

3.2. Uncertainty analysis

Uncertainty analysis was performed to estimate the total values of calculated and measured uncertainties. The uncertainty of measured parameters is a function of systematic errors (i.e. accuracy of the instrument, calibration, and data acquisition) and random errors. The

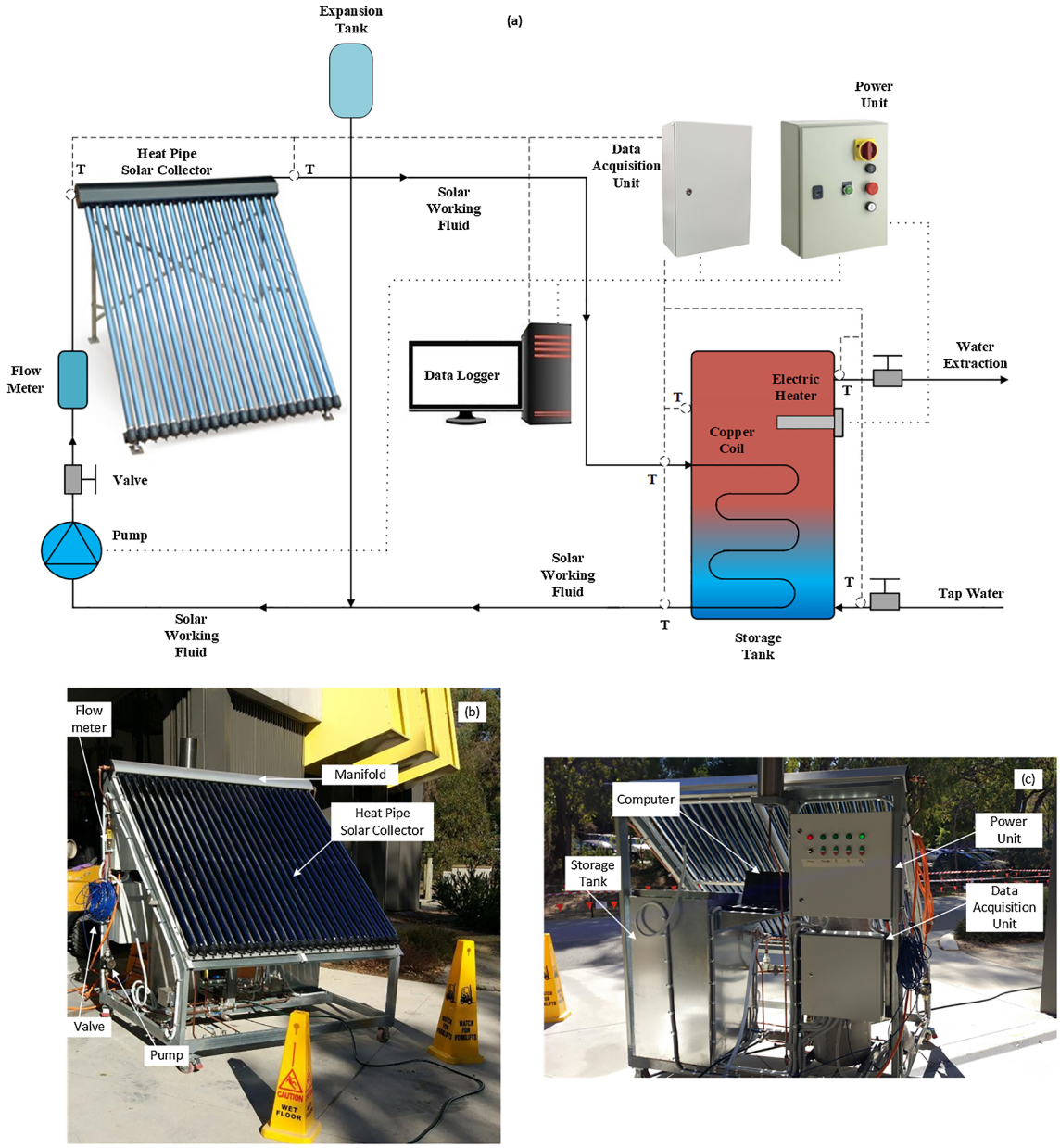

Fig. 3. (a) Schematic of the heat pipe solar water heating system specifically designed, built and used in this study, (b) front view of the experimental setup, and (c) back view of the experimental setup.

Table 1
The specifications of the various components of the heat pipe solar collector.

Solar collector		Glass		Heat pipe	
Number of tubes	25	Transmittance	0.88	Material	Red copper
Tube length (m)	1.80	Thickness (m)	1.60	Condenser Length (m)	0.10
Absorptivity	0.94	Emissivity	0.07	Outer diameter (m)	0.008
Gross area (m^2)	3.93	Outer diameter (m)	0.058		
Insulation	Compressed Rockwool				
Manifold material/diameter (m)	red copper/0.038				

standard deviation method was used to calculate the total uncertainty [36]:

$$W_t = \sqrt{\varepsilon_s{}^2 + \varepsilon_r{}^2} \tag{27}$$

where, W_t is the total uncertainty and ε_s and ε_r are the systematic and random errors, respectively, which can be calculated by [36]:

$$\varepsilon_s = \sqrt{\sum_{i=1}^{n} \varepsilon_{s,i}^2} \tag{28}$$

$$\varepsilon_r = \sqrt{\sum_{i=1}^{n} \varepsilon_{r,i}^2} \tag{29}$$

In abovementioned equations, n is the error source number and $\varepsilon_{r,i}$

Table 2
Results of uncertainty analysis.

Parameter	Type of instrument	Operating range	Systematic uncertainty (± %)	Random uncertainty (± %)	Total uncertainty (± %)
Temperature	Thermocouple: T Type	−185 to 300 °C	1.42	0.32	± 1.7
Flow rate	Flow meter	0–0.068 kg/s	1.34	0.45	2
Solar radiation	Pyranometer (weather station)	0–2000 W/m^2	3	0	3
Wind velocity	Wind speed sensor	0–75 m/s	2.6	0	2.6
Ambient temperature	Air temperature sensor	−20 to 60 °C	1	0	1
Thermal efficiency	–	–	–	–	4.7
Exergy efficiency	–	–	–	–	3.8

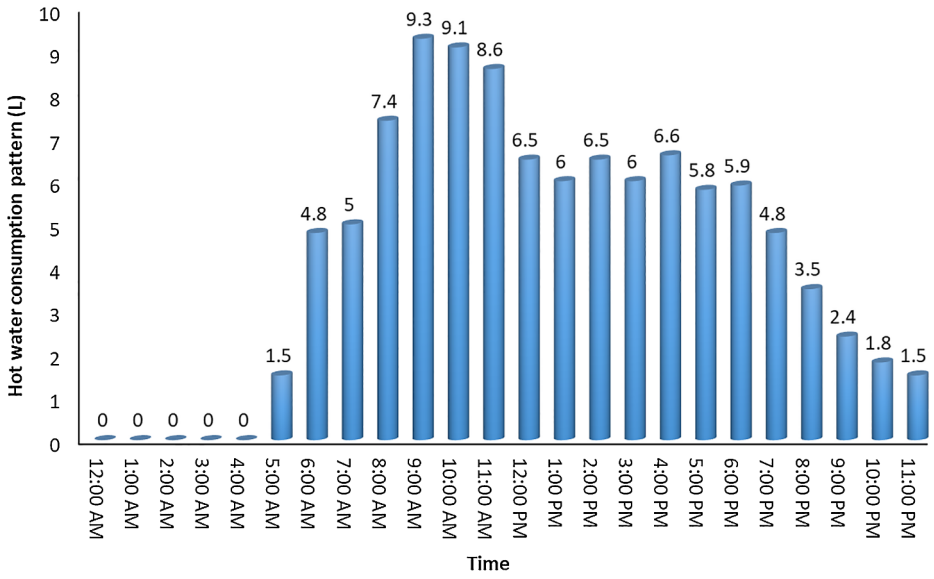

Fig. 4. The average hot water consumption pattern of Perth residents.

can be calculated by [36]:

$$\varepsilon_{r,i} = \sqrt{\frac{\sum_{i=1}^{n} (\varphi_i - \bar{\varphi})^2}{N(N-1)}} \tag{30}$$

where N and $\bar{\varphi}$ are the number of times a parameter is measured and the average value, respectively.

The propagation of errors method was used to estimate the uncertainty of the calculated quantities. According to Holman [37], the uncertainty of the results (W_R) can be calculated from:

$$W_R = \sqrt{\sum_{i=1}^{n} \left(\frac{\partial R}{\partial x_i} W_i \right)^2} \tag{31}$$

where $R = R(x_1, x_2, \ldots, x_n)$.

In Eq. (31), x represents an independent variable and W is the uncertainty in that variable. Table 2 shows various measured and calculated parameters and their related uncertainties.

3.3. Domestic hot water consumption pattern in Perth

The results of the domestic hot water consumption pattern study by Water Corporation of Western Australia [38] were used to extract the hourly hot water consumption pattern (Fig. 4). It is worth noting that there was no thermal data in Western Australia's Water Corporation report. Therefore, to consider the worst case scenario, the temperature of 60 °C, which is almost the highest recommended setting temperature for water heating systems, was considered for this study.

3.4. Weather data

Fig. 5 presents the climatic data on 21 June 2018 in the city of Joondalup, WA which is located 23 km north of Perth central business district. Although the system has been tested in various days, this date was selected as it included several sunny, partly cloudy, mostly cloudy, and overcast periods which is the typical climatic conditions of Perth in cold season. The overall trend of the solar radiation was initially ascending as a function of time and reached its maximum value at around 12:55 PM, thereafter it started to gradually decrease (Fig. 5a). However, due to cloudy conditions, the solar radiation dropped several times during the day when the clouds covered the sun. The most significant drop occurred between 12:10 PM and 12:40 PM when the sky was highly overcast with dense clouds. The wind velocity data during the day are presented in Fig. 5b and the wind velocity was fluctuating between 0 and 6 m/s.

4. Results and discussion

4.1. Optimum number of glass tubes

Based on the averaged climatic data of Joondalup, Western Australia (which is obtained from the weather station database located at Edith Cowan University and presented in Table 3), the temperature distribution of the solar working fluid for different number of glass tubes was theoretically obtained by the developed model and plotted in Fig. 6. The results show that the temperature of the solar working fluid increases as the number of glass tubes increases, however, the temperature increase rate decreases and becomes comparatively insignificant for the number of tubes beyond 25. For instance, the temperature of the working fluid increases by 6.6% as it passes the fifth heat pipe at 10:30 AM. This value reduces to 4.4%, 2.9%, 1.9% 1.2% when the working fluid passes the 10th, 15th, 20th and 25th heat pipes, respectively. Working fluid temperature increase drops to the

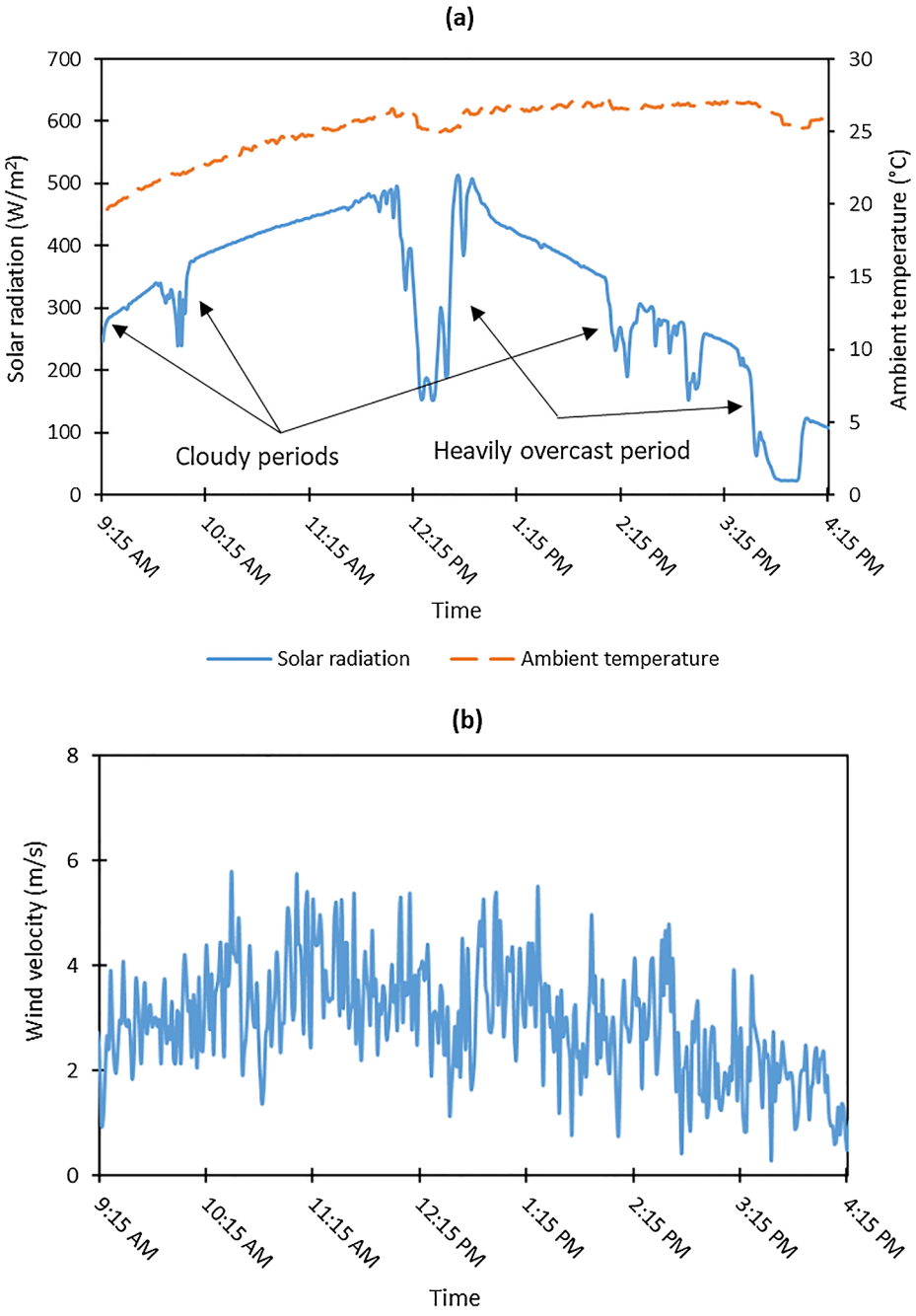

Fig. 5. Climatic conditions on 21 June 2018 in Joondalup: (a) Solar radiation and ambient temperature, (b) Wind velocity.

Table 3
Averaged climatic conditions.

Time	Solar radiation (W/m^2)	Ambient temperature (°C)	Wind velocity (m/s)
9:30 AM	278.3	20.5	2.9
10:30 AM	382.4	23.3	5.8
11:30 AM	435.8	25.1	4.1
1:30 PM	376.7	26.7	3
3:30 PM	295.0	26.8	3.1

insignificant value of 0.6% by increasing the number of heat pipes from 25 to 30.

This behaviour can be explained by the fact that by increasing the number of glass tubes, the overall absorber surface area and consequently the absorbed energy of the collector increases. However, the

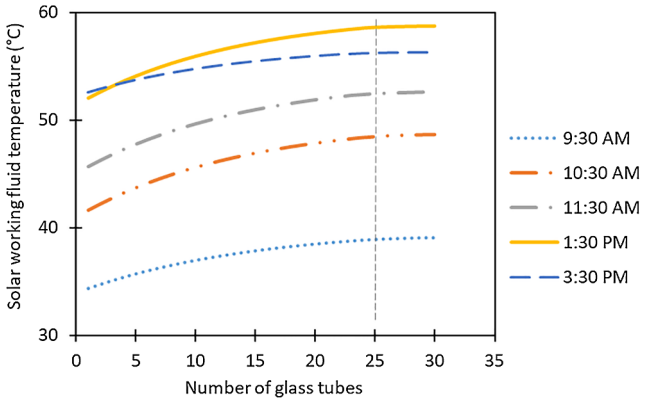

Fig. 6. Solar working fluid temperature versus number of glass tubes.

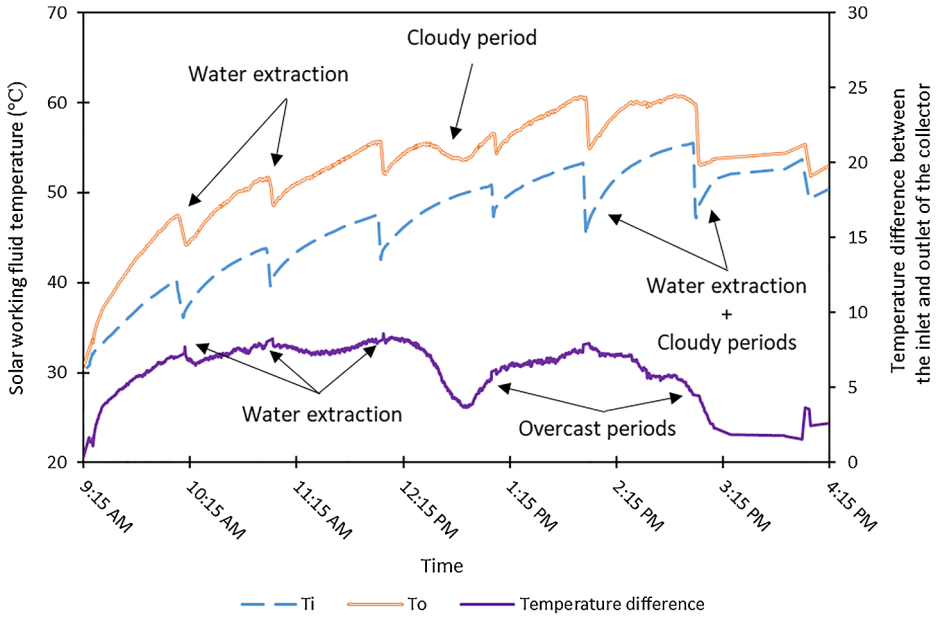

Fig. 7. Variations of the solar working fluid's inlet and outlet temperature and their temperature difference as a function of time on 21 June 2018.

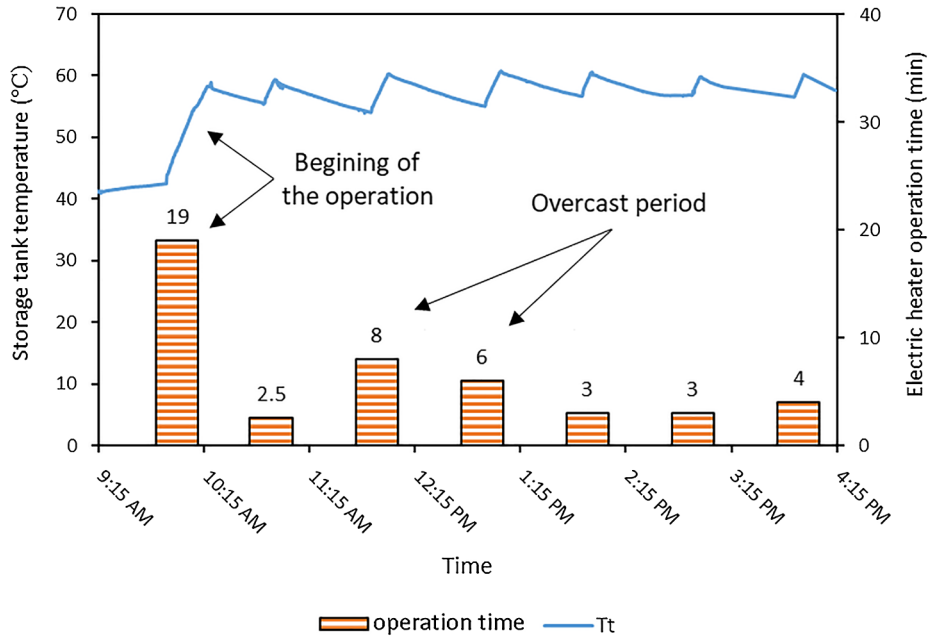

Fig. 8. Temperature variations of water in the storage tank along with the electric heater operation time.

temperature difference between the solar working fluid and heat pipe condenser is maximum at the inlet of the manifold which leads to having the highest heat transfer coefficient and consequently highest heat transfer rate. As the solar working fluid passes through the heat pipes, its temperature increases leading to lower temperature difference between solar working fluid and heat pipe condenser. As a result, the heat transfer rate reduces and the rate of temperature increase diminishes as the number of glass tubes increases.

4.2. Heat pipe solar collector

Fig. 7 shows the inlet and outlet temperature of the solar working fluid (T_i and T_o) along with their temperature difference as a function of time on 21 June 2018. The overall trend of the temperature changes is ascending, however, fluctuations can be seen in the graph which are due to the extraction of hot water to meet the hot water consumption pattern. This water was replaced with tap water from the bottom of the tank which decreased the temperature of the bottom area where the copper coil was located. Consequently, the temperature difference between the solar working fluid (flowing inside the copper coil) and the water inside the tank increased leading to enhanced heat transfer rate between the solar working fluid and water. Therefore, the collector's both inlet temperature (outlet temperature of the copper coil) and outlet temperature dropped. As time passed, the temperature of the water inside the storage tank increased and the heat transfer rate declined. Hence, the outlet temperature of the copper coil (the collector inlet temperature) and the collector outlet temperature continued to increase until the next hot water extraction from the storage tank took place. The data fluctuations in Fig. 7 clearly indicate the importance of considering hot water consumption pattern while analysing the performance of solar heating systems. These fluctuations affect the temperature distribution of the collector inlet and outlet as well as the

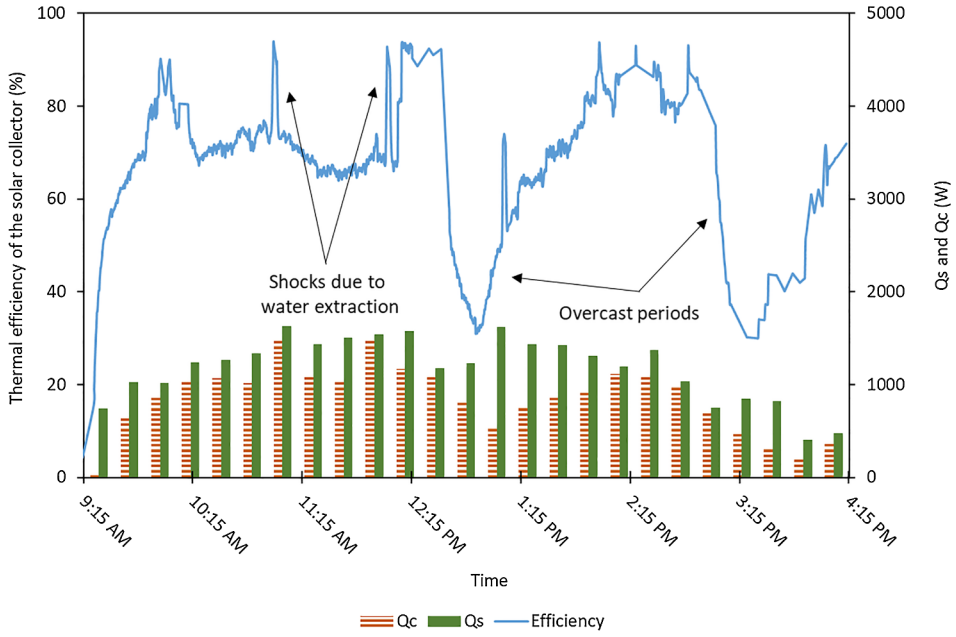

Fig. 9. Thermal efficiency of the heat pipe solar collector along with the available solar energy (Q_s) and the energy transferred to the solar working fluid (Q_c).

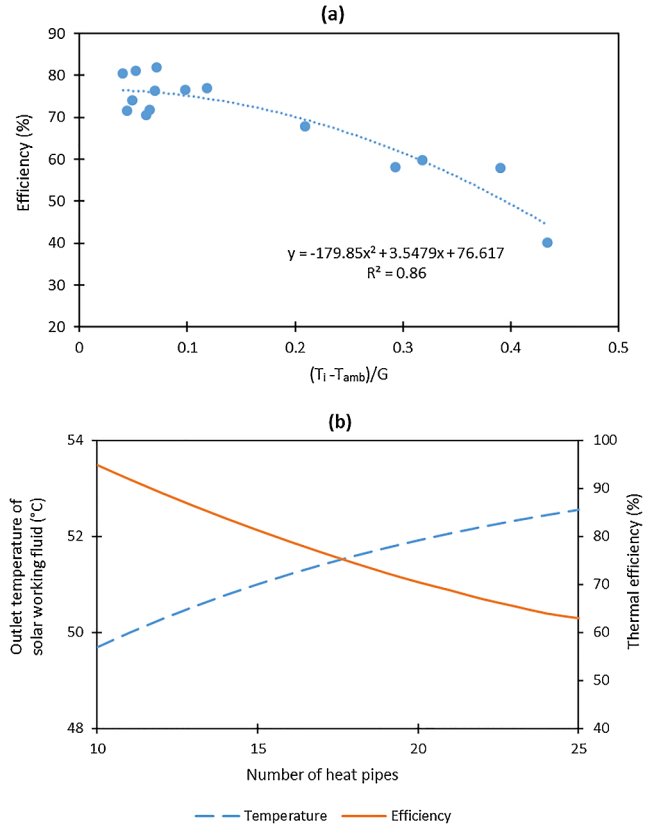

Fig. 10. (a) Efficiency of the heat pipe solar collector as a function of operational and environmental parameters, (b) Temperature changes of the solar working fluid and thermal efficiency as a function of the number of heat pipes.

storage tank and consequently change the amount of absorbed, transferred, and stored thermal energy.

Fig. 7 also shows that the cloudiness has only affected the collector outlet temperature. The reason is that the outlet temperature of the collector relies heavily on the solar radiation while the inlet temperature depends mainly on the temperature of water in the storage tank and hot water consumption pattern. The extraction of water from the storage tank slightly increased the temperature difference while cloudiness significantly lowered it, highlighting that the solar radiation was the major parameter that affected the temperature difference. In addition, when water extraction and cloudy periods coincided (e.g., at 2 or 3 PM), the temperature fluctuations were more severe.

4.3. Water temperature in storage tank

Fig. 8 shows the water temperature variations at top of the storage tank (T_t) along with the auxiliary heater operation time. At the beginning of the day, the solar radiation and water temperature were low and the solar system could not provide all the required energy to increase the water temperature to 60 °C. Therefore, the electric heater was operated for about 19 min which sharply increased the water temperature. By the extraction of hot water, the temperature of water in the storage tank dropped, however, the solar system was able to provide higher amounts of energy due to increased solar radiation which significantly reduced the need for operation of the electric heater (e.g., from 19 to 2.5 min). Therefore, the temperature fluctuations of the storage tank decreased. Due to an overcast period between 11:30 AM to 1 PM, the required operation time of the electric heater increased (from 2.5 min to 8 and 6 min). However, because the system was warmed up and thermal energy had been stored in the storage tank, the increase in the power consumption was not very significant.

4.4. Thermal analysis

The thermal efficiency of the solar collector along with the amount of energy transferred to the solar working fluid (Q_c) and the available solar energy (Q_s) were investigated and the results are presented in Fig. 9. At the beginning of the day, the efficiency of the system was low due to low solar radiation and solar working fluid temperature but it increased with the time. There are two types of fluctuations in Fig. 9, indicating sharp increase and decrease in thermal efficiency. The former was attributed to the hot water extraction which had a positive effect on the overall efficiency of the system. The latter, which had negative impacts on the efficiency, was due to significant reduction of solar radiation during overcast periods.

Analysing the results reveals the positive effect of the water

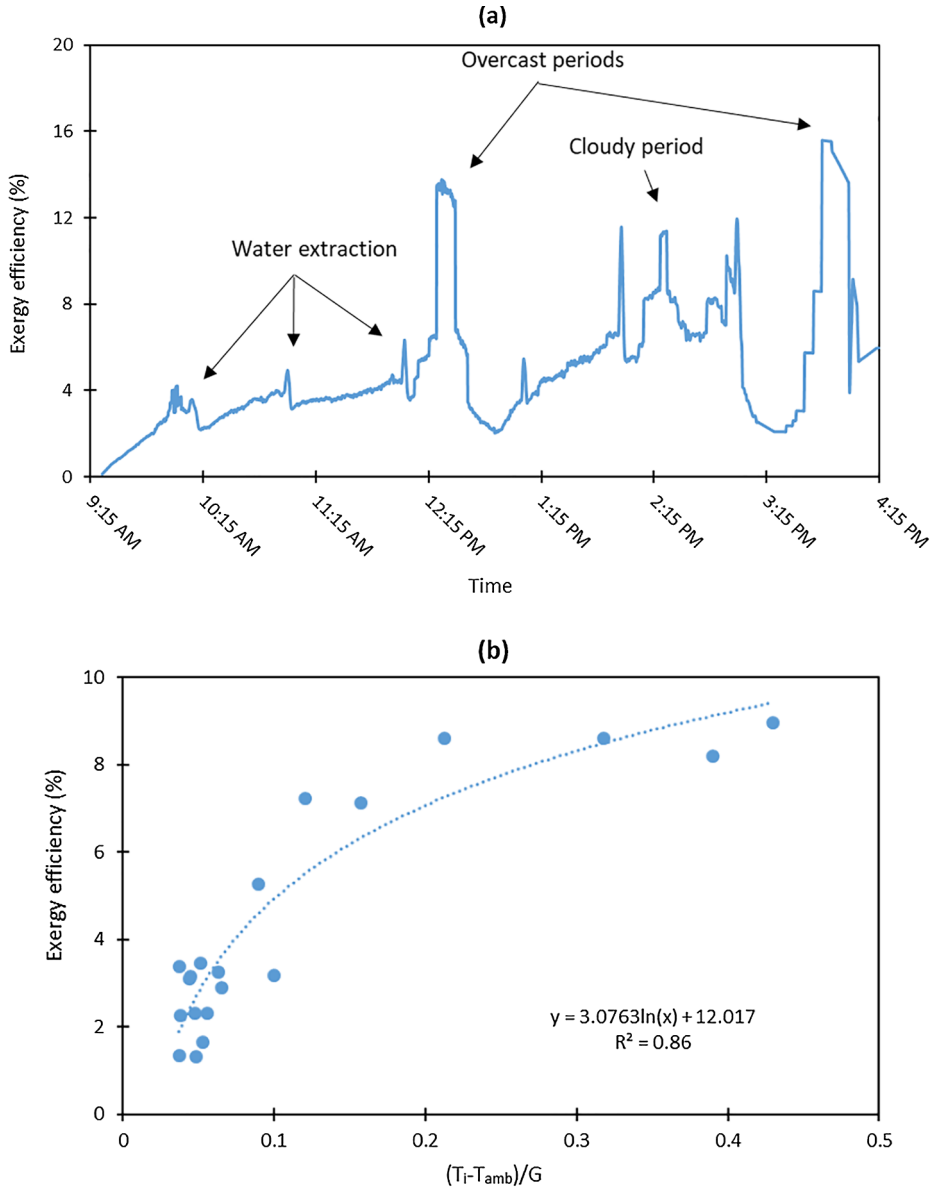

Fig. 11. (a) Exergetic efficiency of the heat pipe solar collector as a function of time, (b) Exergetic efficiency of the heat pipe solar collector as a function of operational and environmental parameters.

extraction on the overall performance of the system. For instance, the amount of the absorbed energy by the solar working fluid was high at around 11 AM because the hot water was being extracted at this time and replaced by tap water, simultaneously. As explained earlier, this decreased the inlet temperature of the collector leading to higher temperature difference between the working fluid and heat pipe condensers, higher heat transfer rate, better usage of available solar energy, and eventually better efficiency. As water extraction stopped, the temperature inside the tank started to rise which increased the inlet temperature of the collector and consequently the amount of absorbed energy by the working fluid decreases (e.g., at 11:13 AM and 11:31 AM). As 12 PM approached, the new round of hot water extraction from the storage tank took place and the same process that occurred at 11 AM was repeated leading to increased amount of the absorbed energy by the working fluid.

Overall, the results suggest that to reach the optimum performance of heat pipe solar water heaters, the amount of hot water extraction should be aligned with the variations of the solar radiation. Hence, a prudent selection of water extraction pattern provides the opportunity to attain higher proportions of available solar energy reflecting greater thermal efficiency.

Fig. 10a indicates the efficiency of the heat pipe solar collector as a function of operational and environmental parameters (i.e. collector inlet temperature (T_i), ambient temperature (T_{amb}), and solar radiation (G)). Solar radiation and ambient temperature are the two most influential climatic parameters and inlet temperature of the collector relies heavily on the operational aspect of the solar system. The results show that the best correlation to describe the experimental data is a second degree polynomial equation of $y = -179.85x^2 + 3.479x + 76.617$ with R^2 value of 0.86, where x and y represent $\frac{T_i - T_{amb}}{G}$ and thermal efficiency, respectively. The experimental data in this study has been recorded in every 10 s which equals to thousands of data sets. To make the regression graphs presentable, a computer program was written and data with almost equal x and y axis values were removed.

Based on this correlation, decreasing the temperature difference between the inlet working fluid and the environment has a positive effect on the system's thermal efficiency. This is mainly due to the fact that lowering the temperature difference decreases the thermal losses of

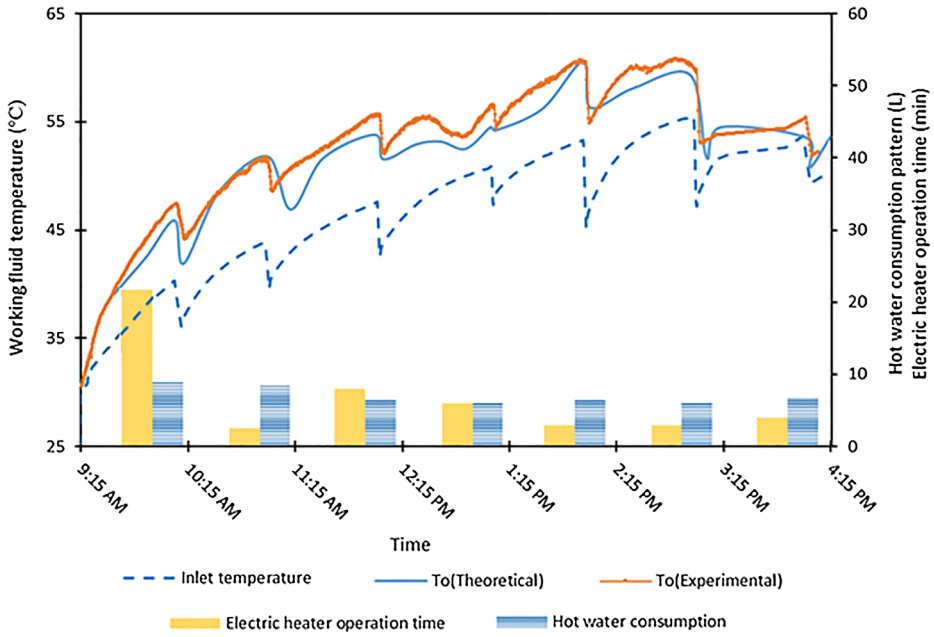

Fig. 12. Theoretical and experimental comparison of the collector outlet temperature.

the solar collector and also increases the amount of the absorbed energy resulting in higher collector outlet temperature. In addition, higher solar radiation leads to higher efficiency if the inlet temperature of the collector is lowered. This emphasises that for applications in which water extraction pattern can be controlled, aligning the hot water extraction pattern with the solar radiation as a method of keeping the inlet temperature of the collector low is very important.

Fig. 10b depicts the theoretical temperature changes of the solar working fluid inside the manifold along with the thermal efficiency under climatic conditions of 11:30 AM. As expected, by increasing the number of heat pipes, the temperature of the solar working fluid increased but with the cost of efficiency reduction. The temperature increase of the solar working fluid not only increased heat loss, but also decreased the temperature difference between the solar working fluid and heat pipe condenser sections, leading to lower heat transfer rate and thermal efficiency. This again proves the importance of finding the optimum number of glass tubes in heat pipe solar water heating systems as discussed in Section 4.1.

4.5. Exergy analysis

Fig. 11a shows the exergetic efficiency of the heat pipe solar collector as a function of time. The overall trend of the exergy efficiency changes is ascending with time, however, there are significant fluctuations in the results, reflecting noticeable increase of exergy efficiency during overcast and cloudy periods. The reason is that the solar radiation was low and the ambient temperature dropped during these periods while the collector inlet and outlet temperatures were still either high or moderate. In addition, exergy destruction decreased upon hot water extraction from the solar system due to the increased temperature difference between collector inlet and outlet which had a positive effect of the exergy efficiency. Moreover, the highest irreversibility occurred at the beginning of the day. Overall, it can be concluded that any strategy which can increase the collector inlet and outlet temperature difference has a positive effect on the exergy efficiency.

Fig. 11b depicts the exergetic efficiency of the heat pipe solar collector as a function of operational and environmental parameters with y and x representing efficiency and $(T_i - T_{amb})/G$, respectively. The results obtained from the regression analysis revealed that the best correlation to describe the experimental data is the logarithmic equation of $y = 3.0763\ln(x) + 12.017$ with R^2 equal to 0.86, where x and y represent $\frac{T_i - T_{amb}}{G}$ and exergy efficiency, respectively. It can be noticed that higher solar radiation leaded to higher ambient temperature which leaded to higher exergy destruction. Also, having higher collector inlet and outlet temperature reduces the thermal losses of the system which contributes to decrease the exergy destruction.

4.6. Model validation

Fig. 12 compares the outlet temperature of the heat pipe solar collector obtained from the developed mathematical model and real experiments. The overall trend of both graphs are almost the same. The maximum absolute difference between the theoretical and experimental values is 5.6% with the standard error of 1.77%. The results of the error analysis indicate the capability of the developed model to predict the thermal performance of heat pipe solar collectors.

4.7. Effect of solar working fluid mass flow rate

Fig. 13 shows the effect of solar working fluid mass flow rate on the outlet temperature (T_o), amount of transferred energy to the solar working fluid (Q_c), and thermal efficiency of the heat pipe solar collector, which were obtained from the theoretical model, at 10 AM, 12 PM, and 2 PM. The climatic conditions at these times are presented in Fig. 5. Decreasing the mass flow rate increased the outlet temperature, however it reduced the amount of absorbed energy and thermal efficiency. Depending on the application, if higher temperature is needed, the absorbed energy and thermal efficiency should be overlooked to some extent and vice versa.

Analysing the results also showed that at high mass flow rates, the thermal efficiency of the solar collector was higher at 12 PM compared to 10 AM and 2 PM, while at low mass flow rates, this parameter had lower values at this time. This is due to the fact that solar radiation was higher at 12 PM and at high solar radiations, higher amounts of thermal energy were available. Therefore, higher mass flow rates provide this opportunity to attain higher amounts of the available energy. Overall, regulating the solar working fluid mass flow rate with solar radiation improves the performance of the system significantly.

To conclude, all these parameters (i.e. solar working fluid mass flow

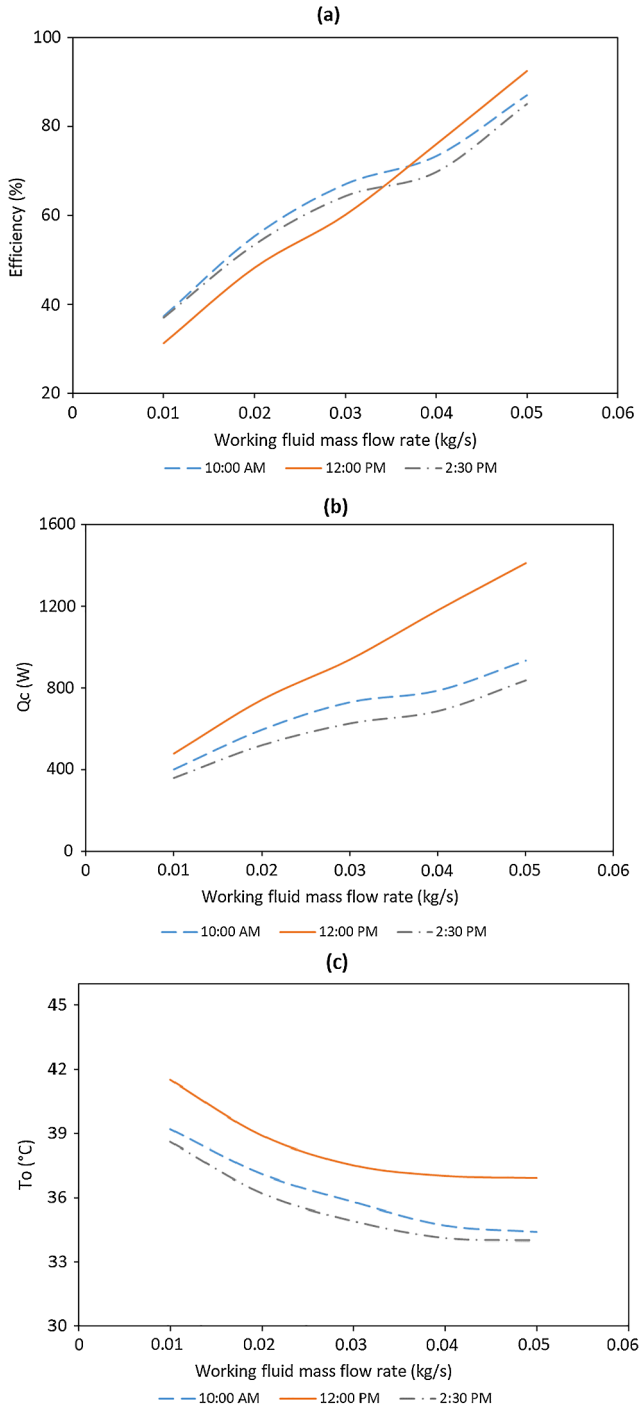

Fig. 13. Effect of solar working fluid mass flow rate on: (a) the thermal efficiency, (b) absorbed energy, and (c) the outlet temperature of the heat pipe solar collector.

rate, collector outlet temperature, amount of absorbed energy, and thermal efficiency) should be considered simultaneously while a solar system is designed.

5. Conclusion

This study was conducted to analyse the cold season thermal performance of a HPSC in a heat pipe solar water heating system under climatic conditions of Perth in Western Australia considering the hot water consumption pattern. The following results were obtained:

- The hot water consumption pattern significantly influences the temperature distribution of the solar collector and the storage tank. Hence, considering hot water consumption pattern plays a crucial role in optimum design of solar water heating systems.
- Hot water extraction has a positive effect on the thermal efficiency of the system while low solar radiation significantly reduces the system efficiency. In addition, the highest exergy destruction occurs at the beginning of the day.
- Decreasing the solar working fluid's mass flow rate has a positive effect on the outlet temperature of the heat pipe solar collector, however it reduces the amount of absorbed energy and thermal efficiency. Also, regulating the solar working fluid mass flow rate with solar radiation improves the performance of the system significantly.
- The developed model in this study well predicts the thermal performance of heat pipe solar collectors.
- A study to investigate the effect of applying selective hot water patterns to find the optimum hot water production capability of the system is highly recommended for future research.
- Optimization of solar working fluid mass flow rate and regulating it with the climatic conditions to achieve the optimum performance of the system is highly recommended for further research.

References

[1] H. Jouhara, A. Chauhan, T. Nannou, S. Almahmoud, B. Delpech, L. Wrobel, Heat pipe based systems - Advances and applications, Energy 128 (2017) 729–754.
[2] R. Singh, S. Kumar, M. Hasan, M. Khan, G. Tiwari, Performance of a solar still integrated with evacuated tube collector in natural mode, Desalination 318 (2013) 25–33.
[3] R. Daghigh, A. Shafieian, Energy and exergy evaluation of an integrated solar heat pipe wall system for space heating, Sādhanā 41 (2016) 877–886.
[4] R. Daghigh, A. Shafieian, An experimental study of a heat pipe evacuated tube solar dryer with heat recovery system, Renew. Energy 96 (2016) 872–880.
[5] Y. Deng, Z. Quan, Y. Zhao, L. Wang, Z. Liu, Experimental research on the performance of household-type photovoltaic-thermal system based on microheat-pipe array in Beijing, Energy Convers. Manage. 106 (2015) 1039–1347.
[6] R. Daghigh, A. Shafieian, Theoretical and experimental analysis of thermal performance of a solar water heating system with evacuated tube heat pipe collector, Appl. Therm. Eng. 103 (2016) 1219–1227.
[7] B. Du, E. Hu, M. Kolhe, An experimental platform for heat pipe solar collector testing, Renew. Sust. Energy Rev. 17 (2013) 119–125.
[8] B. Rassamakin, S. Khairnasov, V. Zaripov, A. Rassamakin, O. Alforova, Aluminum heat pipes applied in solar collectors, Sol. Energy 94 (2013) 145–154.
[9] T. Brahim, M. Dhaou, A. Jemni, Theoretical and experimental investigation of plate screen mesh heat pipe solar collector, Energy Convers. Manage. 87 (2014) 428–438.
[10] R.J. Xu, X.H. Zhang, R.X. Wang, S.H. Xu, H.S. Wang, Experimental investigation of a solar collector integrated with a pulsating heat pipe and a compound parabolic concentrator, Energy Convers. Manage. 148 (2017) 68–77.
[11] D.N. Nkwetta, M. Smyth, Performance analysis and comparison of concentrated evacuated tube heat pipe solar collectors, Appl. Energy 98 (2012) 22–32.
[12] D.N. Nkwetta, M. Smyth, Comparative field performance study of concentrator augmented array with two system configurations, Appl. Energy 92 (2012) 800–808.
[13] D.N. Nkwetta, M. Smyth, The potential applications and advantages of powering solar air-conditioning systems using concentrator augmented solar collectors, Appl. Energy 89 (2012) 380–386.
[14] M.A. Ersoz, Effects of different working fluid use on the energy and exergy performance for evacuated tube solar collector with thermosyphon heat pipe, Renew. Energy 96 (2016) 244–256.
[15] L. Wei, D. Yuan, D. Tang, B. Wu, A study on a flat-plate type of solar heat collector with an integrated heat pipe, Sol. Energy 97 (2013) 19–25.
[16] Y. Deng, Y. Zhao, W. Wang, Z. Quan, L. Wang, D. Yu, Experimental investigation of performance for the novel flat plate solar collector with micro-channel heat pipe array (MHPA-FPC), Appl. Therm. Eng. 54 (2013) 440–449.
[17] S.S. Kumar, K.M. Kumar, S.R.S. Kumar, Design of evacuated tube solar collector with heat pipe, Mater. Today: Proc. 4 (2017) 12641–12646.
[18] X. Zhang, X. Zhao, J. Xu, X. Yu, Characterization of a solar photovoltaic/loop-heat-pipe heat pump water heating system, Appl. Energy 102 (2013) 1229–1245.
[19] W. He, X. Hong, X. Zhao, X. Zhang, J. Shen, J. Ji, Theoretical investigation of the thermal performance of a novel solar loop-heat-pipe façade-based heat pump water heating system, Energy Build. 77 (2014) 180–191.
[20] L. Ayompe, A. Duffy, Thermal performance analysis of a solar water heating system with heat pipe evacuated tube collector using data from a field trial, Sol. Energy 90 (2013) 17–28.
[21] C. Porras-Prieto, F. Mazarro, V. Mozos, J. Garcia, Influence of required tank water temperature on the energy performance and water withdrawal potential of a solar water heating system equipped with a heat pipe evacuated tube collector, Sol. Energy 110 (2014) 365–377.

[22] M. Naghavi, K. Ong, I. Badruddin, M. Mehrali, M. Silakhori, H. Metselaar, Theoretical model of an evacuated tube heat pipe solar collector integrated with phase change material, Energy 91 (2015) 911–924.
[23] P. Feliński, R. Sekret, Effect of PCM application inside an evacuated tube collector on the thermal performance of a domestic hot water system, Energy Build. 152 (2017) 558–567.
[24] A. Shafieian, M. Khiadani, A. Nosrati, A review of latest developments, progress, and applications of heat pipe solar collectors, Renew. Sust. Energy Rev. 95 (2018) 273–304.
[25] E.K. Akpinar, F. Koçyiğit, Energy and exergy analysis of a new flat-plate solar air heater having different obstacles on absorber plates, Appl. Energy 87 (2010) 3438–3450.
[26] E. Azad, Theoretical and experimental investigation of heat pipe solar collector, Exp. Therm. Fluid Sci. 32 (2008) 1666–1672.
[27] Z. Wang, Z. Duan, X. Zhao, M. Chen, Dynamic performance of a facade-based solar loop heat pipe water heating system, Sol. Energy 86 (2012) 1632–1647.
[28] S. Riffat, X. Zhao, P. Doherrty, Developing of a theoretical model to investigate thermal performance ofa thin membrane heat pipe solar collector, Appl. Therm. Eng. 25 (2005) 899–915.
[29] J.H.I. Lienhard, J.H.V. Lienhard, DOE Fundamentals Handbook: Thermodynamics, Heat Transfer, and Fluid Flow, US Department of Energy, Washington DC, 2008.
[30] R. Daghigh, A. Shafieian, Energy-exergy analysis of a multipurpose evacuated tube heat pipe solar water heating-drying system, Exp. Therm. Fluid Sci. 78 (2016) 266–277.
[31] P.D. Dunn, D.A. Reay, Heat pipes, fourth ed., Elsevier Science Ltd., 1994.
[32] T.L. Bergman, A.S. Lavine, F.P. Incropera, D.P. DeWitt, Introduction to Heat Transfer, seventh ed., John Wiley and Sons, New York, 2012.
[33] S.W. Chi, Heat pipe theory and practice, McGraw-Hill, New York, 1976.
[34] B. Bienert, Heat pipes for solar collectors, in: Proceedings of the 1st International Heat Pipe Conference, Stuttgart, Germany 1973.
[35] H. Gunerhan, A. Hepbasli, Exergetic modeling and performance evaluation of solar water heating systems for building applications, Energy Build. 39 (2007) 509–516.
[36] R.J. Moffat, Describing the uncertainties in experimental results, Exp. Ther. Fluid Sci. (1988) 3–17.
[37] J.P. Holman, Experimental methods for engineers, eighth ed., McGraw-Hill, 2011.
[38] M. Loh, P. Coghlan, Domestic water use study in perth, Water Corporation of WA, Western Australia, 2003.